RSC Advances

PAPER

View Article Online
View Journal | View Issue

Cite this: *RSC Adv.*, 2023, **13**, 24854

Effect of granulation on chlorine-release behavior during municipal solid waste incineration

Xinlei Xie, [a] Wei Wu,*[b] Jiali Fu,[a] Linwen Di,[a] Changsheng Bu,[a] Guiling Xu,[a] Junguang Meng, [a] Guilin Piao[a] and Xinye Wang *[ac]

The preparation of refuse-derived fuel (RDF) is an effective and simple means of rural municipal solid waste utilization. The release of chlorine during RDF combustion is important as it causes high-temperature corrosion and pollutants emission such as HCl, dioxins, *etc.* In this paper, constant-temperature and increasing-temperature combustion experiments were carried out using an electrically heating furnace to analyse the effects of granulation (pressure and additives) on the release of chlorine in particles. During the constant-temperature combustion below 800 °C, only organic chlorine was released from the RDF. The increase of granulation pressure from 1 MPa to 10 MPa did not affect the total amount of chlorine release, but delayed the organic chlorine release by increasing the gas diffusion resistance. During the constant-temperature combustion above 900 °C, inorganic chlorine was released as well. The increase of granulation pressure enhanced the inorganic chlorine release significantly by promoting the reactants contact. During the increasing-temperature combustion, the increase of granulation pressure delayed the organic chlorine release as well but inhibited the inorganic chlorine release. This was mainly attributed to the slow temperature rise to 900 °C, during which the inherent calcium in the RDF reacted with silicon and aluminium, resulting in less reactants for an inorganic chlorine release reaction. Three calcium-based additives were used to inhibit chlorine release. $CaCO_3$ showed no dechlorination effect, and CaO showed better dechlorination effect than $Ca(OH)_2$. For the constant-temperature combustion at 900 °C, the addition of CaO with a Ca/Cl ratio of 2 achieved a dechlorination efficiency of over 90%, with little influence from the granulation pressure. For the increasing-temperature combustion, the granulation pressure had a significant influence on CaO dechlorination effectiveness. Only at a granulation pressure as high as 10 MPa, did the addition of CaO with the Ca/Cl ratio of 2.5 achieve a dechlorination efficiency of 95%.

Received 11th July 2023
Accepted 14th August 2023

DOI: 10.1039/d3ra04615j

rsc.li/rsc-advances

1 Introduction

Incineration reduces the volume and harm of urban municipal solid waste (urban MSW) quickly, and generates electricity or heat, making it widely used in many countries, such as China, Japan, South Korea, Singapore, Sweden, *etc.*[1–3] In the cities with high population density and large per capita waste generation, large-scale incineration plants are used with a processing capacity as high as 200–1000 t per day.[4] If the large-scale incineration plant was built in the rural areas with dispersed population and low per capita waste generation, it would result in a large radius of waste collection and the increase of costs in collection, transportation and storage, without any economic feasibility. Therefore, small-scale incineration plants constructed with small-scale incinerators align better with the generation characteristics of rural municipal solid waste (rural MSW). The processing capacity of small-scale incinerators usually ranges from 10–100 t per day, and are not equipped with power generator for their low thermal efficiency and low energy output, resulting in the low economic viability. Moreover, if the complete flue gas purification system, equipped in large-scale incineration plants, was equipped, it would further increase operational costs and reduces economic feasibility, thereby burden the local finances.

To address these issues, we proposed the construction of a rural MSW treatment center in the junction areas of several villages, which encompasses granulation, storage and incineration, as illustrated in Fig. 1. The wastes from each village are collected and transported to the treatment center. Firstly, the wastes are subjected to coarse crushing and sorted manually and magnetically to remove foreign matters and iron. Subsequently, the wastes are finely crushed and sorted magnetically again. The remaining waste is then compress to high-density refuse-derived fuel (RDF) using a granulator. Finally, the RDF

[a]*Jiangsu Provincial Key Laboratory of Materials Cycling and Pollution Control, School of Energy and Mechanical Engineering, Nanjing Normal University, Nanjing 210023, China*

[b]*Nanjing Environment Group Co., Ltd, Nanjing 210026, China*

[c]*Zhenjiang Institute for Innovation and Development, Nanjing Normal University, Zhenjiang 212050, China*

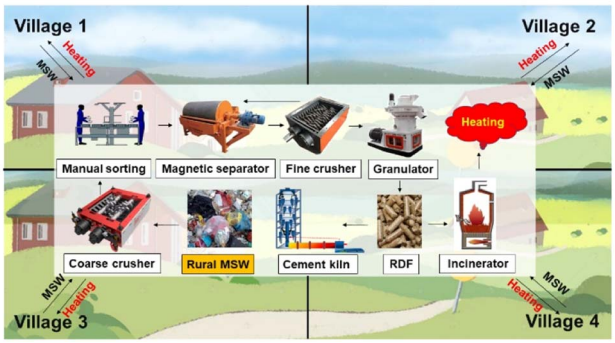

Fig. 1 Process of preparing RDF from rural municipal solid waste.

particles are incinerated in small-scale incinerators to provide heat for the villages. If there are rotary cement kilns or other furnaces near the villages, the incinerators can be omitted, and the RDF particles can be sold to these factories as alternative fuels, with the proceeds going towards village development funds.

The advantages of RDF preparation lie in the following three points. (1) Energy density per unit volume of waste is improved, thereby increasing the heat load in furnace and the efficiencies of combustion and heat transfer. (2) Addition of calcium-based additives, such as $Ca(OH)_2$ and CaO,[5–7] during the granulation inhibits the generation of foul odorous gases from organic matter decay in the waste, reducing storage requirements. (3) Calcium-based additives also inhibit the release of HCl/Cl_2 which can cause the high-temperature corrosion of the heat exchange tubes, produce the air pollution and generate dioxins. HCl/Cl_2 can penetrate the protective oxide layer in the surface of tubes and diffuses through the oxide layer through pores and cracks to react with the metal alloys to form metal chlorides.[8] As the air pollutant, HCl and Cl_2 are not only toxic but also harmful to ozone layer for their catalysis on the decomposition of O_3.[9] Not only in furnace at 500–850 °C but also in flue at 200–500 °C, HCl/Cl_2 provide chlorine for dioxins production by high-temperature gas-phase reaction mechanism and "*de novo*" synthesis mechanism.[10]

The chlorine-release behavior is one of the keys for RDF combustion, which has been studied extensively. Plastics, especially PVC, are considered as the main source of chlorine in MSW.[7] Aracil *et al.*[11] suggested that approximately 38–66% of the chlorine in MSW comes from PVC. In addition to organic chlorides in plastics, there are also inorganic chlorides primarily sourced from kitchen waste. The primary forms of inorganic chlorine are NaCl and KCl. The typical reactions converting organic and inorganic chlorides into HCl are shown in eqn (1)–(3), where Na can be replaced by K.[7] The chlorine release from PVC is believed to occur in two stages, at temperatures of 200–360 °C and 360–500 °C,[12] while NaCl or KCl have higher chlorine release temperatures. Yasuhara *et al.*[13] found that NaCl and KCl in waste volatilized at 800 °C and partially converted into HCl. Kanters *et al.*[14] investigated the conversion of NaCl to HCl and found 55% of NaCl intake was emitted as HCl in 1.5 h at 780 °C, while 40% remained in the sand. Hatanaka *et al.*[15] found that NaCl in waste was converted into HCl in the primary combustion chamber at 700 °C, forming dioxins in the secondary combustion chamber. Additionally, calcium-based additives ($Ca(OH)_2$ and CaO) and magnesium-based additives ($MgCO_3$) are usually used as inhibitors to inhibit chlorine release. Wey *et al.*[16] found that the addition of CaO with 2% of the total waste mass reduced chlorine release by 95% at 600 °C. Wang *et al.*[17] reported a 78% reduction in chlorine release at 740 °C by adding $Ca(OH)_2$ with 3.2% of the total waste mass. Dai *et al.*[18] achieved a 90% reduction in chlorine release at 1000 °C by adding $MgCO_3$ with 10% of the total waste mass consists.

$$\text{PVC: } (CH_2CHCl)_n \rightarrow n\text{HCl} + nC_2H_2 \quad (1)$$

$$\text{NaCl: } 2\text{NaCl} + SO_2 + 0.5O_2 + H_2O \rightarrow Na_2SO_4 + 2\text{HCl} \quad (2)$$

$$\text{NaCl: } 2\text{NaCl} + H_2O + m\text{SiO}_2 \rightarrow Na_2O\cdot m\text{SiO}_2 + 2\text{HCl} \quad (3)$$

In summary, the previous studies have primarily focused on chlorine release characteristics during RDF combustion, with factors such as temperature, time, waste composition, and additives being considered.[19–23] However, there is a lack of research on the impact of RDF particle granulation on chlorine release. The MSW without granulation is loose and the contact between components is insufficient, resulting in the low conversion rate of some solid–solid reactions and gas–solid reactions. Therefore, after granulation, some reactions which generate HCl/Cl_2 or inhibit chlorine release may be enhanced, leading to the changes in chlorine-release behavior. Meanwhile, granulation decreases the voids in MSW and increases the gas diffusion resistance, probably changing in chlorine-release behavior. In addition, the additives addition during granulation should have good dechlorination effect. Therefore, this study aims to comparatively investigate the chlorine-release behavior during the combustion of the RDF granulated at different pressures, to understand the effect and mechanisms of granulation on chlorine-release behavior. The combustion conditions were divided into constant-temperature combustion, simulating the conditions of fluidized bed,[24] and increasing-temperature combustion, simulating the conditions of mechanical grate.[25] Additionally, CaO, $Ca(OH)_2$ and $CaCO_3$ were also used as additives in the granulation process.

2 Materials and methods

2.1 Preparation of RDF

The modeled RDF was prepared using representative components of rural MSW in China as shown in Table 1.[4] The components were divided into biomass (kitchen waste, paper, wood and bamboo, natural textiles) and other materials (dust and bricks, glass, plastics, metals, and other inert materials). After manual sorting and magnetic separation (Fig. 1), most metals were removed from the rural MSW.

Hence, metals were not taken into consideration in RDF. Biomass sawdust was used as a simplified substitute for kitchen waste, paper, wood and bamboo, and textiles. The plastics were

Table 1 RDF components in the experiment

Rural MSW components	Biomass	Dust and brick	Glass	Plastic		Metal	Water
RDF components	Sawdust	Clay	Powdered glass	PVC	PE	None	Deionized water
Particle content (%)	64	14	4	3	6	0	10
Mass in particle (g)	6.4	1.4	0.4	0.3	0.6	0	1.00

classified as PVC which contains chlorine and PE which is chlorine free.

To ensure the uniformity of the prepared RDF, the components above were prepared into powders first. Then, they were uniformly mixed according to the ratio to obtain a total mass of 500 g of mixed powder. Finally, 10 g of the mixture was filled into a cylindrical mold and pressed to the pressures of 1 MPa, 5 MPa and 10 MPa, meeting the low, medium and high granulation pressure requirements for biomass moulding fuels (BMF), respectively. The compression was held for 30 s after reaching the desired granulation pressure. The size of RDF was the diameter of 3 cm and the length of 3 cm.

2.2 Experimental setup

Experimental apparatus for RDF combustion is shown in Fig. 2. Compressed air from an air cylinder was provided to supply the required air for combustion, and its flow rate was controlled by a mass flow meter. The combustion took place in an electric heating furnace with a heated section of 500 mm length and 60 mm diameter. HCl in the flue gas was absorbed in three gas-washing bottles containing deionized water. The first bottle can also collect the condensed water from the flue gas. The quartz tube exposed on the outside of the electric heating furnace, three-way valve, connection pipes and up to the mouth of the HCl absorbing liquid bottle were all equipped with electric heating jackets to maintain a temperature of 120 °C, preventing condensation of water and absorption of HCl that could cause sampling loss. To ensure continuous sampling, two sets of sampling systems were set up, and switching were performed using three-way valve to ensure uninterrupted sampling between the two sets. Three-stage water washing was conducted to ensure the complete absorption of HCl, with the criterion that the chloride ion concentration in the third bottle should be within 1% of the previous stage.

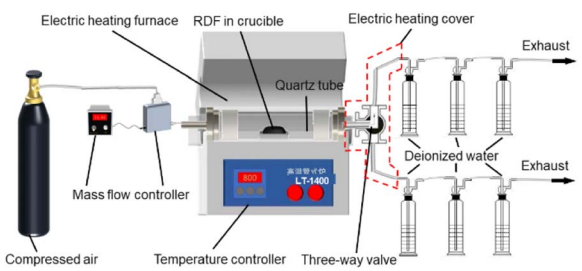

Fig. 2 Experimental system of RDF combustion and gaseous chlorine collection.

The main types of RDF incinerator are fluidized bed incinerator and mechanical grate incinerator, corresponding to constant-temperature and increasing-temperature combustion conditions, respectively. Under constant-temperature combustion conditions, the crucible loaded with RDF was sent directly into the heating zoom at a constant temperature ranged from 700 to 1000 °C. Each sampling duration was 5 min and the total sampling time was 40 minutes. Under increasing-temperature combustion conditions, the crucible loaded with RDF was sent into the heating zoom at 200 °C for 30 min to simulate the drying stage in mechanical grate incinerator. Then, the temperature was raised to 1000 °C at the rate of 10 °C min^{-1} to simulate the combustion stage, and was maintained at 1000 °C for 30 min to simulate the burn-out stage. Finally, the furnace was cooled down to simulate the cooling stage.

To suppress chlorine release, three inexpensive calcium-based compounds (CaO, $Ca(OH)_2$, and $CaCO_3$) were selected as RDF additive which was mixed with the components in Table 2 for its uniform distribution in RDF. Because the molar ratio of Ca/Cl in $CaCl_2$ is 2, the fraction of additive in RDF was designed to follow the Ca/Cl molar ratios of 1.5, 2 and 2.5.

2.3 Analytical methods

After measuring the volume of the absorption solution in each gas-washing bottles by measuring cylinder, 1 mL of the absorption solution was taken and diluted to 50 mL for the chloride ion concentration analysis by the automatic potentiometric titrator (ZDJ-4B) equipped with chloride ion electrode and 0.05 mol L^{-1} $AgNO_3$ solution.

To avoid the chlorine loss during combustion and sampling, the chlorine contents in the samples were analyzed from the perspective of chlorine release.

The chlorine release amounts obtained from the combustion of the components in Table 1 at 1000 °C for 30 min is shown in Table 2. Therefore, the total chlorine content ($Q_{T\text{-}Cl}$) of the 10 g RDF is 57.83 mg. The chlorine release fraction (η_{Cl}) was calculated based on eqn (4) to determine the chlorine recovery fraction.

$$\eta_{Cl} = \left(\frac{Q_{S\text{-}Cl}}{Q_{T\text{-}Cl}}\right) \times 100\% \quad (4)$$

where, $Q_{S\text{-}Cl}$ represents the total amount of chlorine absorbed by the first and second-stage scrubbers during a specific period of time in the RDF combustion process.

Volatilization rate of Cl (β_{Cl}) was calculated according to eqn (5).

Table 2 Chlorine release amounts of different components in RDF

MSW components	Biomass	Dust and brick		Glass	Plastic	
RDF components	Sawdust	Clay		Powdered glass	PVC	PE
Chlorine release amounts (mg g^{-1})[a]	2	0	0		149	0
Chlorine release amounts (mg/RDF)[b]	13.13	0	0		44.70	0
Chlorine release proportion (%)	22.7	0		0	77.3	0

[a] mg g^{-1} refers to the amount of chlorine released per g of the corresponding component. [b] mg/RDF refers to the amount of chlorine released from the corresponding component in an RDF sample, and an RDF particle is 10 g.

$$\beta_{Cl} = \frac{\eta_{Cl}}{t} \quad (5)$$

where, t represents time.

The dechlorination effect (Φ) is defined as eqn (6).

$$\Phi = \left(1 - \frac{\eta_2}{\eta_1}\right) \times 100\% \quad (6)$$

where, η_1 represents the chlorine release fraction without the addition of additives and η_2 represents the chlorine release fraction with the addition of additives under the same granulation pressure and temperature conditions.

3 Results and discussion

3.1 Effect of granulation pressure on chlorine release

3.1.1 Constant-temperature combustion of additive-free RDF. The volatilization rate of Cl during the constant-temperature combustion process of RDF with different intensities of grain is illustrated in Fig. 3. For all conditions, chlorine release reached the maximum release fraction within 10 min and gradually decreases starting from 25 min until it reached a halt at 40 min. Usually, the residence time of RDF in the fluidized bed incinerator is 10–20 min, resulting in some chlorine not being able to volatilize and entering the ash. As the combustion temperature increased, the chlorine release exhibited different characteristics. At the combustion temperature of 700 °C, the maximum volatilization rate of Cl was achieved between 5–10 min, followed by a gradual decrease (Fig. 3a-1). With the granulation pressure increasing, a constant total chlorine release fraction maintained 69% at 40 min which causes a delay in chlorine release (Fig. 3a-2). Before 10 min, the order of chlorine volatilization rate was 1 MPa > 5 MPa > 10 MPa, whereas after 10 min, the order was reversed as 10 MPa > 5 MPa > 1 MPa (Fig. 3a-1). For the combustion at 800 °C, the maximum chlorine volatilization rate occurred earlier, within 0–5 min, and then sharply decreased after 20 min. Compared to the situation at 700 °C, chlorine volatilization rate between 5–20 min was significantly enhanced to that in the condition of 800 °C (Fig. 3b-1). The granulation pressure which was increased at 800 °C did not alter the total chlorine release fraction of 77%. However, it caused

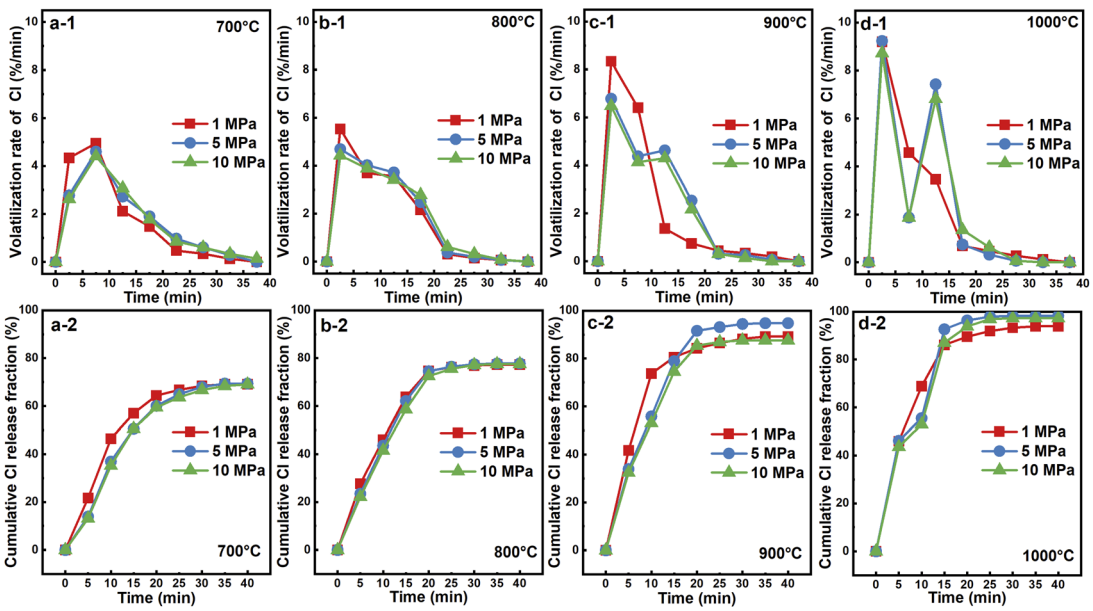

Fig. 3 Volatilization rate (the first row) and cumulative release fraction (the second row) of chlorine during constant-temperature combustion at 700 °C (a), 800 °C (b), 900 °C (c) and 1000 °C (d).

a delay in chlorine release (Fig. 3b-2). The order of volatilization rate before and after 10 min was also reversed.

The volatilization rate of Cl during the combustion of 1 MPa RDF at 900 °C also exhibits a mono-peak characteristic, whereas the volatilization rate of Cl for 5 MPa and 10 MPa RDF combustion showed a dual-peak pattern (Fig. 3c-1). The first peak occurred during 0–5 min, and the second peak occurred during 10–15 min. Increasing the granulation pressure significantly suppresses the chlorine release rate during 0–5 min and promotes the chlorine release during 15 min and 20 min. Furthermore, the increase in granulation pressure also resulted in changes in the total chlorine release fraction (Fig. 3c-2), which was not simply positively or negatively correlated. The corresponding order of granulation pressure was 95% (5 MPa) > 88% (10 MPa) > 87% (1 MPa). A more prominent feature was the release of chlorine under 1000 °C combustion conditions. The chlorine volatilization rate for 1 MPa RDF at 1000 °C still exhibited a mono-peak pattern, whereas the chlorine volatilization rates for 5 MPa and 10 MPa RDF combustion showed a more significant dual-peak pattern (Fig. 3d-1). The chlorine volatilization rate for 5 MPa RDF at 1000 °C combustion after 5 min was 3.3 times higher compared to that at 700 °C combustion after 5 min. The changes in the total chlorine release fraction during combustion at 1000 °C correspond to the following granulation pressure order: 98% (5 MPa) > 97% (10 MPa) > 94% (1 MPa) (Fig. 3d-2).

3.1.2 Increasing-temperature combustion of additive-free RDF. The volatilization rate of Cl during the increasing-temperature combustion of additive-free RDF at various granulation pressures is shown in Fig. 4a. The volatilization rate of Cl for RDF combustion at 1 MPa exhibited a dual-peak characteristic, with the first peak occurring between 40–45 min (300–350 °C) and the second peak at 145 min (1000 °C). For RDF combustion at 5 MPa and 10 MPa, the first peak occurred between 45–50 min (350–400 °C) and 65–70 min (550–600 °C), respectively, while the second peak occurred between 90–100 min (800–900 °C) for both pressures. This suggested that with increasing granulation pressure, the first peak shifted towards higher temperatures, while the second peak shifted towards lower temperatures. In other words, the first peak of chlorine release was delayed, while the second peak of chlorine release was advanced. The cumulative release fraction of chlorine (Fig. 4b) indicated that increasing granulation pressure inhibited chlorine release, contrary to the promoting effect observed under constant-temperature combustion conditions. The total chlorine release fraction during the temperature-rise combustion processed for RDF at 1 MPa, 5 MPa, and 10 MPa were 100%, 96%, and 90%, respectively. All cases showed that chlorine release ended at 140 min during the temperature-rise combustion, because no chlorine release observed during the cooling stage after 1000 °C.

3.2 Mechanisms of mono-peak and dual-peak chlorine releases

Before analyzing the influence of granulation pressure, it is important to understand the basic mechanisms underlying chlorine release in Fig. 3a and 4a. The chlorine present in the RDF used in the experiment mainly originates from organic chlorine in PVC and inorganic chlorine in sawdust (NaCl or KCl). Li *et al.*[26] reported that chlorine release from PVC starts around 225 °C. Wang *et al.*[27] have demonstrated that chlorine release from NaCl initiates at temperatures higher than 800 °C under the influence of SiO_2/Al_2O_3. Therefore, chlorine release during constant-temperature combustion at 700 °C and 800 °C is solely attributed to organic chlorine. However, the cumulative chlorine release fraction at 700 °C was only 69% (Fig. 3b-1), while at 800 °C, it reaches 77% (Fig. 3b-2), consistent with the proportion of organic chlorine shown in Table 2. This suggested that at 700 °C, some of the organic chlorine was absorbed, while at 800 °C, all of it was released. The XRD analysis of clay, which acted as a substitute for brick tiles and dust in RDF composition (Fig. 5), revealed a significant presence of $CaCO_3$. Therefore, it is speculated that HCl was partially absorbed by $CaCO_3$ to form $CaCl_2$ (eqn (6)). Since the melting point of $CaCl_2$ is 772 °C, it did not volatilize at 700 °C and remained in the residue (Fig. 5). However, at a temperature

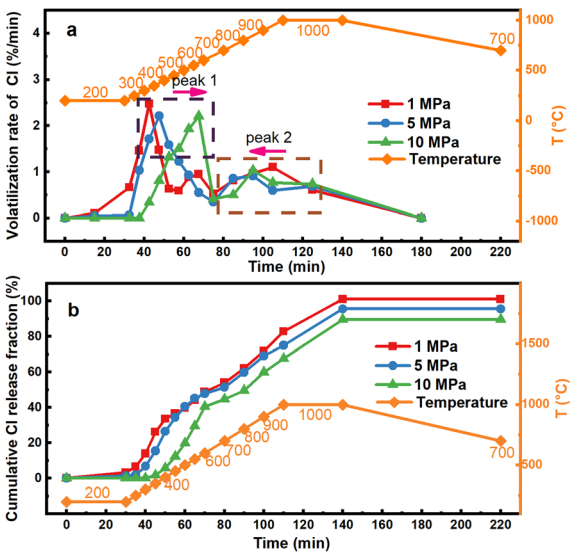

Fig. 4 Volatilization rate (a) and cumulative release fraction (b) of chlorine during increasing-temperature combustion.

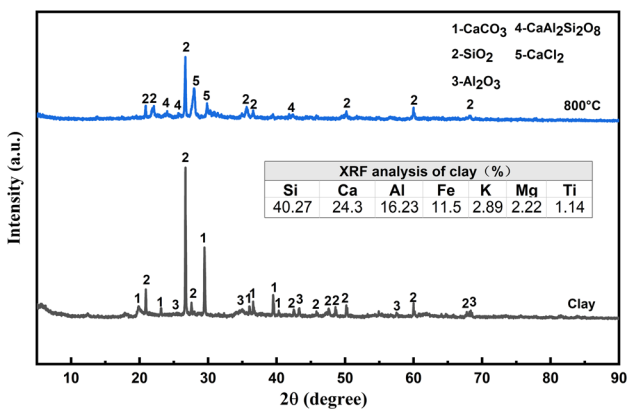

Fig. 5 XRD patterns of clay component and RDF combustion products.

exceeding 800 °C, $CaCl_2$ can volatilize into the gas phase. Research by Fraissler *et al.*[28] has shown that $CaCl_2$ can react with O_2, H_2O, and CO_2 to release HCl (eqn (7)–(10)). Due to the relatively slow rates of these reactions compared to the decomposition of PVC into HCl, the increased chlorine release at 800 °C mainly occurred during the 10–20 min period, appearing as a gradual process without a distinct peak. The above explanation provides insight into the mechanism underlying mono-peak chlorine release.

$$2HCl + CaCO_3 \rightarrow CaCl_2 + H_2O + CO_2 \quad (7)$$

$$CaCl_2 + 0.5O_2 \rightarrow CaO + Cl_2 \quad (8)$$

$$CaCl_2 + CO_2 + 0.5O_2 \rightarrow CaCO_3 + Cl_2 \quad (9)$$

$$CaCl_2 + H_2O \rightarrow CaO + 2HCl \quad (10)$$

$$CaCl_2 + H_2O + CO_2 \rightarrow CaCO_3 + 2HCl \quad (11)$$

At combustion temperatures of 900 °C and 1000 °C, the theoretical temperatures for the release of chlorine-containing gases from NaCl[29] and KCl (eqn (12)–(17)) are achieved. Therefore, the release of inorganic chlorine during the 10–20 min period is further enhanced, resulting in a significant second peak of chlorine release. The mechanism behind the dual-peak chlorine release during temperature-rise combustion is similar to that observed during constant-temperature combustion. The second peak of chlorine release is primarily attributed to organic chlorine at lower temperatures and to inorganic chlorine at higher temperatures.

$$NaCl + SiO_2 + O_2 \rightarrow Na_xSi_yO_z + Cl_2 \quad (12)$$

$$NaCl + Al_2O_3 + O_2 \rightarrow Na_xAl_yO_z + Cl_2 \quad (13)$$

$$NaCl + SiO_2 + Al_2O_3 + O_2 \rightarrow Na_wSi_xAl_yO_z + Cl_2 \quad (14)$$

$$NaCl + SiO_2 + H_2O \rightarrow Na_xSi_yO_z + HCl \quad (15)$$

$$NaCl + Al_2O_3 + H_2O \rightarrow Na_xAl_yO_z + HCl \quad (16)$$

$$NaCl + SiO_2 + Al_2O_3 + H_2O \rightarrow Na_wSi_xAl_yO_z + HCl \quad (17)$$

3.3 Influencing mechanisms of granulation pressure on chlorine release

3.3.1 Delaying effect of granulation on chlorine release. During constant-temperature combustion at 700 °C and 800 °C (Fig. 3a-1 and b-1), the chlorine release was delayed due to the increase in granulation pressure, while the total amount of chlorine released remained unchanged. The morphological changes of RDF particles during constant-temperature combustion at 800 °C are shown in Fig. 6. At 10 min, the RDF particles exhibited cracking. However, the regions outside the cracks remained cylindrical in shape. Although the degree of RDF particle cracking continued to increase, some particles still maintained a cylindrical shape until 25 min. At the end of the 45 minute combustion, the RDF particles showed multiple fractures. This indicates that the increase in granulation pressure reduced the internal voids of the RDF particles, thereby increasing the diffusion resistance of HCl outward in the RDF, resulting in a slow release of HCl. At the same time, the RDF particles continued to crack during combustion, leading to a continuous decrease in this resistance. The delayed release of chlorine observed during the temperature ramp from 200 °C to 700 °C can also be explained by the increased diffusion resistance.

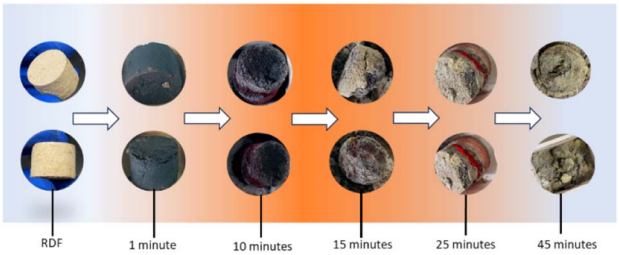

Fig. 6 Morphological changes of RDF during constant-temperature combustion at 800 °C.

3.3.2 Promoting effect of granulation on chlorine release. During constant-temperature combustion conditions, the promoting effect of the increasing granulation pressure on chlorine release was shown at 900 °C and 1000 °C (Fig. 3c-2 and d-2), rather than at 700 °C and 800 °C (Fig. 3a-2 and b-2). The main difference between the chlorine release at 900 °C and 1000 °C and that at 700 °C and 800 °C is the inorganic chlorine release in the former condition, not in the latter condition. Therefore, the increase of granulation pressure was considered to promote the release of inorganic chlorine. During the combustion of the RDF granulated at 1 MPa, there is no second peak caused by the release of inorganic chlorine, while it is observed during the combustion of the RDF granulated at 5 MPa and 10 MPa. This indicates that the contact between NaCl/KCl and SiO_2 and Al_2O_3 in the clay component (Fig. 5) was weak during the combustion of the RDF granulated at 1 MPa, resulting in the slight reactions as eqn (12)–(17). Whereas, the granulation of RDF at 5 MPa and 10 MPa caused better contact between the reactants, significantly enhancing the reactions. Wang *et al.*[27] suggested that NaCl participates in the reactions in gaseous form in eqn (12)–(17). Therefore, when the granulation pressure increases, the diffusion resistance of NaCl from the interior to the exterior of the RDF increases, prolonging the residence time of NaCl in the RDF and promoting its reaction with SiO_2. Additionally, the increased granulation pressure also reduced the voids within the RDF particles, resulting in a more uniform distribution of NaCl vapor within the particles. As a result, the increased granulation pressure enhances the contact time and contact area between the gas-phase and solid-phase reactants.

The second peak in the volatilization rate of chlorine observed during increasing-temperature combustion (Fig. 4a) is also attributed to the release of inorganic chlorine. The increased granulation pressure enhances the chlorine release

reactions of inorganic chlorine, leading to an earlier appearance of the peak.

3.3.3 Inhibiting effect of granulation on chlorine release. The increase in granulation pressure during the increasing-temperature combustion process resulted in the suppression of chlorine release, contrary to the promoting effect during constant-temperature combustion process. During the organic chlorine release process (0–70 min, Fig. 4b), although the 5 MPa granulation pressure led to a delay in chlorine release, it did not significantly reduce the total amount, indicating a primarily physical diffusion hindering effect. However, when the granulation pressure increased to 10 MPa, the total organic chlorine release from 0–70 min decreased from 49% (1 MPa RDF) to 41%. Therefore, it promoted the reaction between $CaCO_3$ and HCl when the granulation pressure further increased to 10 MPa. However, as shown in eqn (7)–(11), $CaCl_2$ can still release HCl and Cl_2. Therefore, during the organic chlorine release stage, the pressure only delays the release process.

The cumulative proportion of chlorine release from 5 MPa RDF combustion started to be lower than that of 1 MPa RDF combustion, until the end of combustion when the combustion temperature during the temperature increase exceeded 900 °C (Fig. 4b). This indicates that the increase in granulation pressure suppresses the inorganic chlorine release during the increasing-temperature combustion process. In contrast, the increase in granulation pressure promotes the inorganic chlorine release during the 900 °C and 1000 °C constant-temperature combustion processes. Obviously, these differences in effects are caused by temperature differences. During the 900 °C constant-temperature combustion process, the RDF heating rate is greater than 50 °C s^{-1}, and the residence time below 900 °C is less than 20 s. During the increasing-temperature combustion process, the RDF heating rate is 0.17 °C s^{-1} (10 °C min^{-1}). The residence time below 900 °C is 5400 s. Therefore, there is sufficient time during the increasing-temperature combustion below 900 °C. The decomposition of $CaCO_3$ starts from 700 °C, producing CaO.[30] Trubitsyn *et al.*[31] found that CaO can react with Al_2O_3 to form $Ca_{12}Al_{14}O_{33}$ at 430 °C. Mazzucato *et al.*[32] found that CaO can react with SiO_2 at temperatures as low as 700 °C. XRD analysis of the residue of RDF heated at 800 °C for 30 min (Fig. 5) showed no $CaCO_3$ and the presence of $CaSi_2Al_2O_8$. Therefore, under increasing-temperature combustion conditions, before 900 °C, the CaO produced from the decomposition of $CaCO_3$ in RDF reacts with SiO_2 and Al_2O_3, consuming some of the SiO_2 and Al_2O_3 that could have reacted with NaCl to release inorganic chlorine, resulting in less inorganic chlorine release compared to constant-temperature combustion. The increase in granulation pressure promotes the solid–solid contact and reaction between CaO, SiO_2, and Al_2O_3, further suppressing the release of inorganic chlorine.

3.4 Effect of additives on chlorine release

3.4.1 Constant-temperature combustion of RDF with additive. The dechlorination effect of the additives during constant-temperature combustion at 900 °C are shown in Fig. 7. Clay in the RDF already contains a significant amount of $CaCO_3$ (Fig. 5), which is believed to reduce chlorine release. However, the addition of additional $CaCO_3$ (Ca/Cl = 1.5) did not show any chlorination absorption effect. Therefore, the $CaCO_3$ present in the RDF is considered to be excessive, and the addition of additional $CaCO_3$ is ineffective. On the other hand, CaO and $Ca(OH)_2$ effectively suppressed chlorine release, with CaO showing better results. Within the range of Ca/Cl ratios of 1.5–2.5, $Ca(OH)_2$ showed similar dechlorination efficiencies, ranging from 28% to 46%. Among the CaO additives, those with Ca/Cl ratios of 2 and 2.5 showed similar and the highest dechlorination efficiencies (1 MPa ~90%, 5 MPa ~93%, 10 MPa ~94%), while the CaO additive with a Ca/Cl ratio of 1.5 had significantly lower dechlorination efficiencies (62–75%), but still higher than the dechlorination efficiency of $Ca(OH)_2$ with a Ca/Cl ratio of 2.5. The granulation pressure had little effect on the dechlorination efficiency.

The volatilization rate and cumulative release fraction of chlorine in RDF combustion with additives at a constant temperature of 900 °C are shown in Fig. 8. The addition of CaO and $Ca(OH)_2$ reduces the first peak of chlorine release and eliminates the second peak of chlorine release (Fig. 8b-1 and c-1). When $Ca(OH)_2$ with a Ca/Cl ratio of 2.5 is used as an additive, the cumulative chlorine release fraction is reduced to 49% (1 MPa RDF), 52% (5 MPa RDF), and 52% (10 MPa RDF). When CaO with a Ca/Cl ratio of 2 is used as an additive, the cumulative chlorine release fraction is reduced to 10% (1 MPa RDF), 8% (5 MPa RDF), and 5% (10 MPa RDF).

3.4.2 Increasing-temperature combustion of RDF with additive. Due to the optimal dechlorination effect exhibited by CaO, RDF with direct addition of CaO was chosen for investigation during increasing-temperature combustion, and the results are shown in Fig. 9. Both the granulation pressure and the amount of CaO which were increased significantly increase the dechlorination efficiency. At granulation pressures of 1 MPa and 5 MPa, the dechlorination efficiency of CaO with a Ca/Cl ratio of 2.5 was only 64% and 78%, respectively, which is much lower than the dechlorination efficiency during constant-temperature combustion. Only at a granulation pressure of 10 MPa, the dechlorination efficiency of CaO with a Ca/Cl ratio of 2.5 reached 95%.

The volatilization rate and cumulative release fraction of chlorine in RDF combustion with additives during increasing-

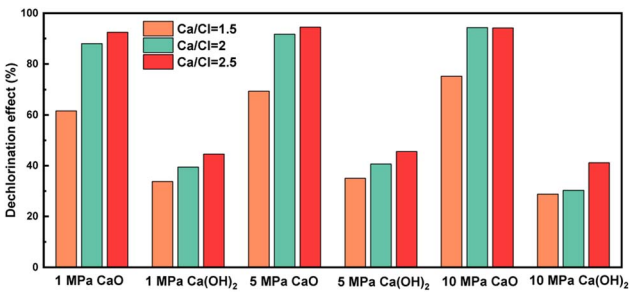

Fig. 7 Dechlorination effect of additives during constant-temperature combustion at 900 °C.

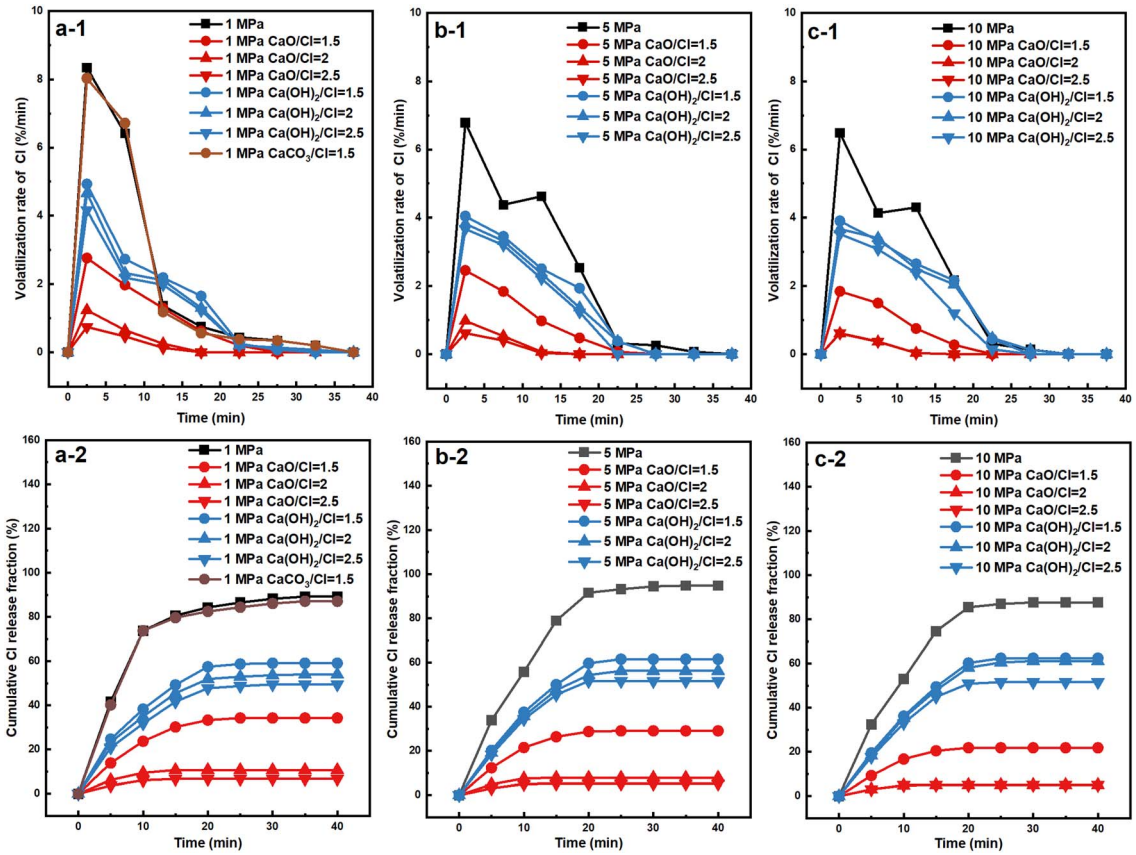

Fig. 8 Volatilization rate (the first row) and cumulative release fraction (the second row) of chlorine with additives at a constant temperature of 900 °C and the granulation pressures of 1 MPa (a), 5 MPa (b) and 10 MPa (c).

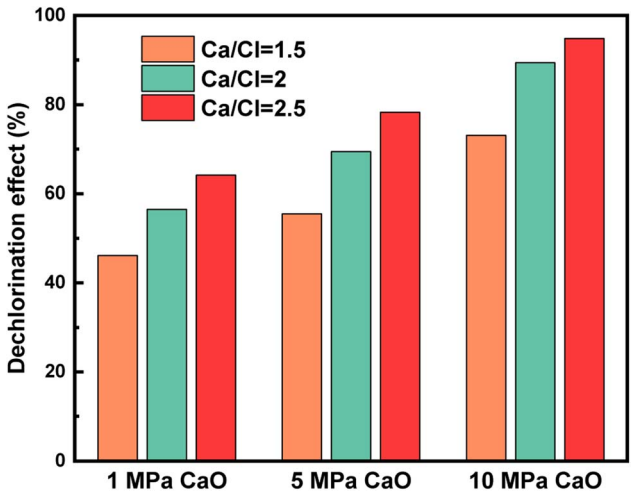

Fig. 9 Dechlorination effect of additives during increasing-temperature combustion.

temperature combustion condition are shown in Fig. 10. The addition of CaO reduces the release peaks of organic chlorine and inorganic chlorine. Increasing the granulation pressure also enhances the inhibitory effect of CaO on the release of organic chlorine and inorganic chlorine. When CaO with a Ca/Cl ratio of 2.5 is used as an additive, the cumulative chlorine release fraction is reduced to 36% (1 MPa RDF), 21% (5 MPa RDF), and 5% (10 MPa RDF).

3.5 Influencing mechanisms of additives on chlorine release

3.5.1 Dechlorination mechanisms of CaO and $Ca(OH)_2$. The addition of CaO and $Ca(OH)_2$ reduced the first peak of chlorine release and eliminated the second peak of chlorine release (Fig. 8b-1 and c-1). This indicates that CaO and $Ca(OH)_2$ not only absorb the HCl released from organic chlorine, but also inhibit the chlorine release of inorganic chlorine. The absorption of HCl by CaO and $Ca(OH)_2$ is a simple acid–base neutralization reaction. They inhibit the chlorine release of inorganic chlorine through two pathways. One is the absorption of HCl and Cl_2 released from inorganic chlorine at high temperatures, resulting in the formation of $CaCl_2$. The other is the consumption of some SiO_2 and Al_2O_3 by the additives, reducing their reaction with NaCl. The XRD spectrum of the combustion residue (Fig. 11) also reveals the presence of $CaCl_2$ and $CaAl_2Si_2O_8$.

3.5.2 The reason why CaO performs better than $Ca(OH)_2$. Wey *et al.*[16] and Dou *et al.*[33] reported that the dechlorination effect of CaO is superior to $Ca(OH)_2$. In the experimental preparation process, deionized water accounted for 10% of the total RDF, while the added CaO only accounted for a maximum of 1.77% of the total RDF. The theoretical

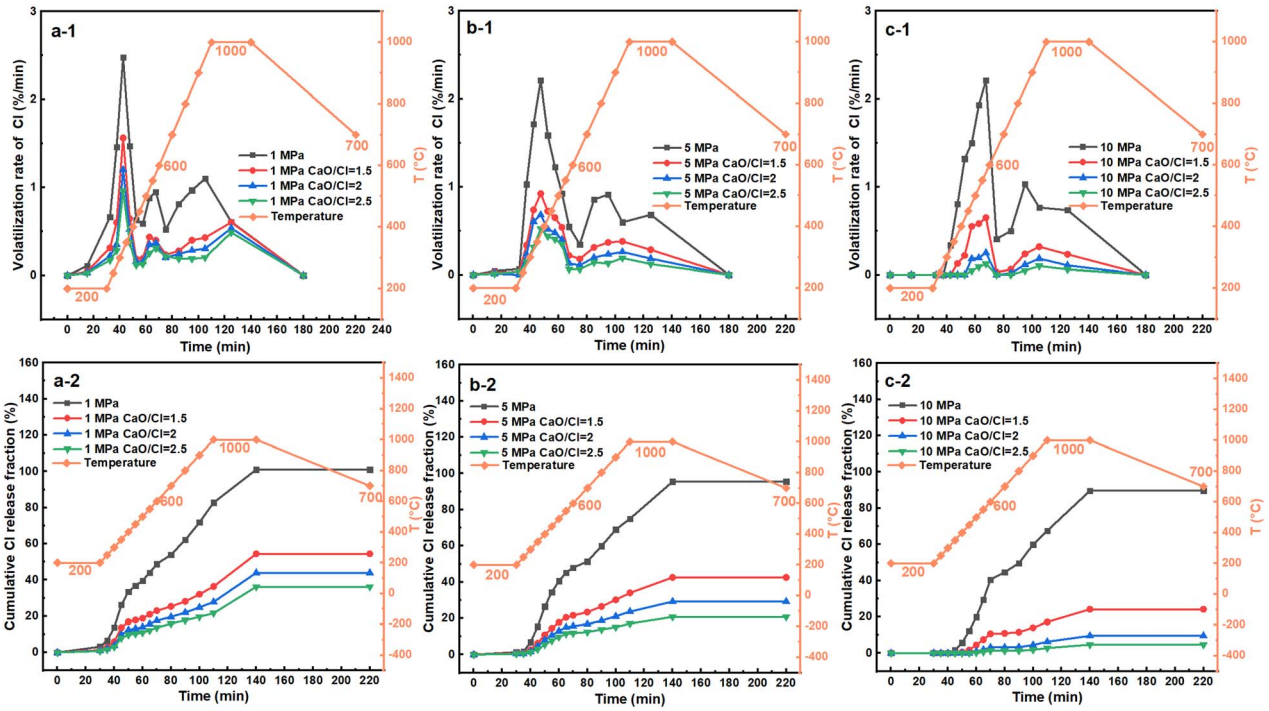

Fig. 10 Volatilization rate (the first row) and cumulative release fraction (the second row) of chlorine during increasing-temperature combustion of RDF with additives at the granulation pressures of 1 MPa (a), 5 MPa (b) and 10 MPa (c).

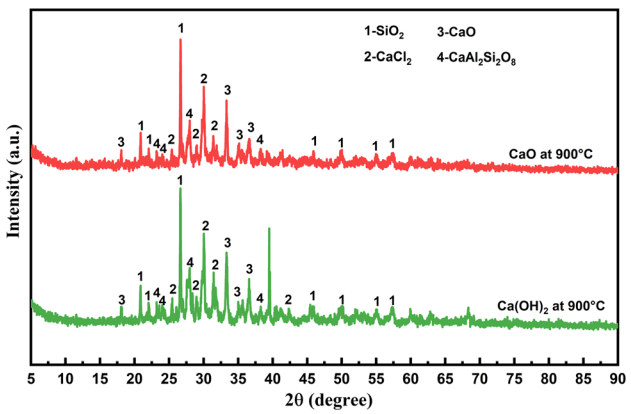

Fig. 11 XRD pattern of RDF combustion products with additives.

proportion of $Ca(OH)_2$ produced by the reaction of CaO and H_2O was 2.33% of the total RDF, which only required 5.7% of the total deionized water added to the RDF to fully react. The water content in the RDF was much higher than the amount of water required for the reaction of $Ca(OH)_2$ with CaO. During the granulation process, CaO and water in the RDF came into close contact, and most of the CaO was converted into $Ca(OH)_2$, while the remaining unreacted CaO reacted with the water generated during drying and combustion of the RDF to further form $Ca(OH)_2$. At this point, due to the required temperature and humidity, the molar volume of $Ca(OH)_2$ was approximately twice that of CaO, similar to steam activation.[34–36] Therefore, the additive expanded and formed a large number of cracks, reconstructed the pore structure and particle surface, thereby enhancing the dechlorination effect. Subsequently, $Ca(OH)_2$ decomposed back into CaO at high temperatures, breaking the chemical bonds in the hydroxide ions, creating the second set of pores. Finally, CaO reacted with HCl to produce $CaCl_2$ and H_2O, forming hydrogen bonds and creating the third set of pores. These repeated pore formations weaken the decrease in dechlorination effect caused by the agglomeration of CaO at high temperatures, enhance the non-catalytic gas–solid reaction between CaO and HCl, and thereby enhance the dechlorination effect of CaO. On the other hand, $Ca(OH)_2$ only undergoesed two sets of pore changes.[37] Additionally, CaO can directly react with HCl and Cl to form $CaCl_2$, while $Ca(OH)_2$ typically decomposes into metal oxides at high temperatures and then reacts with chlorine to generate $CaCl_2$. Therefore, the dechlorination effect of $Ca(OH)_2$ was inferior to CaO.

4 Conclusions

The effects of granulation pressure and additives on chlorine release in RDF particles were analyzed by the constant-temperature and increasing-temperature combustion experiments. Under constant-temperature combustion conditions not exceeding 800 °C, only organic chlorine was released from the RDF with the chlorine release fractions less than 77%. The granulation pressure which was increased from 1 MPa to 10 MPa did not affect the total chlorine release but delayed the release of organic chlorine by increasing gas diffusion

resistance. When the constant-temperature combustion was above 900 °C, both organic and inorganic chlorine started to be released with the chlorine release fractions higher than 87%. The increase in granulation pressure promoted reactant contact, resulting in a significant enhancement of inorganic chlorine release. Under increasing-temperature combustion conditions, the chlorine release fractions were higher than 89%. The increase of granulation pressure also delayed the release of organic chlorine but suppressed the release of inorganic chlorine. This is mainly due to the slow temperature rise before 900 °C, during which the inherent calcium compound in RDF reacted with silicon and aluminium, reducing the reactants required for inorganic chlorine release. Three calcium-based additives were used to inhibit chlorine release, with $CaCO_3$ showing no dechlorination effect, and CaO exhibiting better dechlorination effect than $Ca(OH)_2$. During the constant-temperature combustion at 900 °C, the addition of CaO with a Ca/Cl ratio of 2 achieved a dechlorination efficiency higher than 90%, with little influence from granulation pressure. During the increasing-temperature combustion, granulation pressure had a significant influence on CaO dechlorination effectiveness. Only at a granulation pressure of 10 MPa, the addition of CaO with a Ca/Cl ratio of 2.5 could achieve a dechlorination efficiency of 95%.

Author contributions

Xinlei Xie: investigation, visualization, writing – original draft; Wei Wu: conceptualization, methodology; Jiali Fu and Linwen Di: investigation; changsheng Bu, Guiling Xu, Junguang Meng and Guilin Piao: data curation, formal analysis, validation, funding acquisition; Xinye Wang: conceptualization, methodology, writing – review & editing, supervision, funding acquisition.

Conflicts of interest

There are no conflicts to declare.

Acknowledgements

This work was financially supported by the National Key R&D Program of China (No. 2022YFE0206600), the National Natural Science Foundation of China (No. 52176115) and the the Natural Science Foundation of Jiangsu Province (No. BK20200733).

Notes and references

1 N. Ogawa, T. Amano and Y. Koike, *J. Mater. Cycles Waste Manage.*, 2021, **23**, 158–164.
2 H. Cheng and Y. Hu, *Bioresour. Technol.*, 2010, **101**, 3816–3824.
3 C. Brereton, *Resour., Conserv. Recycl.*, 1996, **16**, 227–264.
4 H. Zhou, A. Meng, Y. Long, Q. Li and Y. Zhang, *Renewable Sustainable Energy Rev.*, 2014, **36**, 107–122.
5 Y.-C. Chen and Y.-C. Tsai, *Sci. Total Environ.*, 2022, **841**, 156745.
6 K. Liu, W. P. Pan and J. T. Riley, *Fuel*, 2000, **79**, 1115–1124.
7 W. C. Ma, G. Hoffmann, M. Schirmer, G. Y. Chen and V. S. Rotter, *J. Hazard. Mater.*, 2010, **178**, 489–498.
8 H. P. Nielsen, F. J. Frandsen, K. Dam-Johansen and L. L. Baxter, *Prog. Energy Combust. Sci.*, 2000, **26**, 283–298.
9 S. J. Yin, X. Yi, L. Li, L. Huang, M. C. G. Ooi, Y. J. Wang, D. T. Allen and D. G. Streets, *ACS Earth Space Chem.*, 2022, **6**(7), 1846–1857.
10 S. C. Chen, L. Yu, C. M. Zhang, Y. F. Wu and T. Y. Li, *J. Environ. Manage.*, 2023, **339**, 117942.
11 I. Aracil, R. Font and J. A. Conesa, *J. Anal. Appl. Pyrolysis*, 2005, **74**, 465–478.
12 I. C. McNeill, L. Memetea and W. J. Cole, *Polym. Degrad. Stab.*, 1995, **49**, 181–191.
13 A. Yasuhara, T. Katami, T. Okuda, N. Ohno and T. Shibamoto, *Environ. Sci. Technol.*, 2001, **35**, 1373–1378.
14 M. J. W. Kanters, R. v. Nispen, R. Louw and P. Mulder, *Environ. Sci. Technol.*, 1996, **30**, 2121–2126.
15 T. Hatanaka, T. Imagawa, A. Kitajima and M. Takeuchi, *Environ. Sci. Technol.*, 2001, **35**, 4936–4940.
16 M.-Y. Wey, J.-C. Chen, H.-Y. Wu, W.-J. Yu and T.-H. Tsai, *Fuel*, 2006, **85**, 755–763.
17 Z. Q. Wang, H. T. Huang, H. B. Li, C. Z. Wu, Y. Chen and B. Q. Li, *Energy Fuels*, 2002, **16**, 608–614.
18 M. Q. Dai, Z. S. Yu, Y. T. Tang and X. Q. Ma, *J. Energy Inst.*, 2020, **93**, 1036–1044.
19 M. Zajemska, P. Rajca, S. Szwaja and S. Morel, *Przem. Chem.*, 2019, **98**, 907–910.
20 X. Wei, Y. Wang, D. Liu, H. Sheng, W. Tian and Y. Xiao, *Energy Fuels*, 2009, **23**, 1390–1397.
21 G. Piao, K. Hakamada, M. Kondoh, M. Yamaguchi, R. Yamazaki, S. Hatano and S. Mori, *Kagaku Kogaku Ronbunshu*, 2000, **26**, 551–556.
22 Z. Liu, H.-q. Wang, Y.-y. Zhou, X.-d. Zhang and J.-w. Liu, *Waste Manage. Res.*, 2017, **35**, 757–765.
23 T. Hase, M. A. Uddin, Y. Kato, M. Fukui and Y. Kanao, *Energy Fuels*, 2014, **28**, 6475–6480.
24 J. Peters, J. May, J. Stroehle and B. Epple, *Energies*, 2020, **13**(18), 4665.
25 N. Razmjoo, H. Sefidari and M. Strand, *Fuel Process. Technol.*, 2016, **152**, 438–445.
26 W. Li, Z. Q. Bai, T. T. Zhang, Y. X. Jia, Y. J. Hou, J. Chen, Z. X. Guo, L. X. Kong, J. Bai and W. Li, *Fuel*, 2023, **340**, 127555.
27 X. Y. Wang, H. Xie, R. Du, Y. Y. Liu, P. F. Lin, J. B. Zhang, C. S. Bu, Y. J. Huang and W. Zhang, *RSC Adv.*, 2018, **8**, 34449–34458.
28 G. Fraissler, M. Joller, T. Brunner and I. Obernberger, *Chem. Eng. Process.*, 2009, **48**, 380–388.
29 D. He, H. Hu, F. Jiao, W. Zuo, C. Liu, H. Xie, L. Dong and X. Wang, *Chem. Eng. J.*, 2023, **467**, 143344.
30 W. Yue, W. Song, C. Fan and S. Li, *Chem. Eng. Sci.*, 2023, **273**, 118646.
31 M. A. Trubitsyn, L. V. Furda, M. N. Yapryntsev and N. A. Volovicheva, *Russ. J. Inorg. Chem.*, 2022, **67**, 1308–1318.

32 E. Mazzucato and A. F. Gualtieri, *Phys. Chem. Miner.*, 2000, **27**, 565–574.
33 W. Duo, N. F. Kirkby, J. P. K. Seville, J. H. A. Kiel, A. Bos and H. Den Uil, *Chem. Eng. Sci.*, 1996, **51**, 2541–2546.
34 V. Manovic, D. Lu and E. J. Anthony, *Fuel*, 2008, **87**, 3344–3352.
35 A. Coppola, L. Palladino, F. Montagnaro, F. Scala and P. Salatino, *Energy Fuels*, 2015, **29**, 4436–4446.
36 V. Manovic and E. J. Anthony, *Environ. Sci. Technol.*, 2007, **41**, 1420–1425.
37 Y. Wang, W. Su, J. Chen, Y. Xing, H. Zhang and D. Qian, *Environ. Sci. Pollut. Res.*, 2023, **30**, 73116–73136.